Conjugating Phosphospermines to siRNAs for Improved Stability in Serum, Intracellular Delivery and RNAi-Mediated Gene Silencing

ARTICLE *in* MOLECULAR PHARMACEUTICS · NOVEMBER 2012

Impact Factor: 4.38 · DOI: 10.1021/mp300278b · Source: PubMed

molecular pharmaceutics

Article

pubs.acs.org/molecularpharmaceutics

Conjugating Phosphospermines to siRNAs for Improved Stability in Serum, Intracellular Delivery and RNAi-Mediated Gene Silencing

Clément Paris,[†] Valérie Moreau,[†] Gaëlle Deglane,[†] Loukmane Karim, Bernard Couturier, Marie-Elise Bonnet, Valérie Kedinger, Mélanie Messmer, Anne-Laure Bolcato-Bellemin, Jean-Paul Behr, Patrick Erbacher,* and Nathalie Lenne-Samuel

Polyplus-tranfection SA, Bioparc, Boulevard S. Brant, Illkirch, 67401, France

Supporting Information

ABSTRACT: siRNAs are usually formulated with cationic polymers or lipids to form supramolecular particles capable of binding and crossing the negatively charged cell membrane. However, particles hardly diffuse through tissues when administered *in vivo*. We therefore are developing cationic siRNAs, composed of an antisense sequence annealed to an oligophosphospermine-conjugated sense strand. Cationic siRNAs have been previously shown to display gene silencing activity in human cell line (Nothisen et al. *J. Am. Chem. Soc.* **2009**). We have improved the synthesis, purification and characterization of oligospermine-oligoribonucleotide conjugates which provide cationic siRNAs with enhanced biological activity. We show data supporting their carrier-free intracellular delivery in a molecular, soluble state. Additional results on the relationship between global charge, uptake and silencing activity confirm the requirement for an overall positive charge of the conjugated siRNA in order to enter cells. Importantly, conjugated siRNAs made of natural phosphodiester nucleotides are protected from nuclease degradation by the oligophosphospermine moiety, operate through the RNAi mechanism and mediate specific gene silencing at submicromolar concentration in the presence of serum.

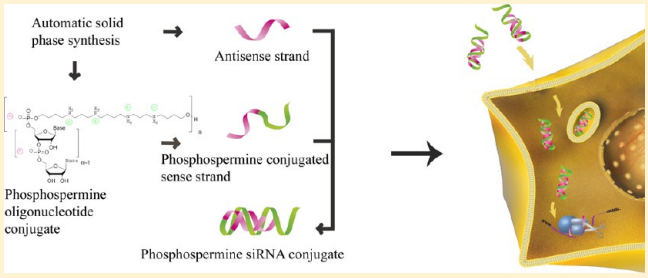

KEYWORDS: *oligonucleotide conjugate, siRNA delivery, ZNA, spermine*

INTRODUCTION

Thanks to their unprecedented potency to post-transcriptionally turn off the expression of any target gene in tissue culture,[1] small interfering RNAs (siRNAs) have allowed researchers to make inestimable advances in understanding biological processes over the past decade. Mechanistically, synthetic siRNAs, which are 19−23 base-pair duplexes, exploit the cellular RNAi pathway which has the function to naturally regulate gene expression. In plants and invertebrates, it is also a mechanism of defense against pathogens.[2] siRNAs are loaded by the cellular RISC complex, which triggers duplex unwinding and selection of the antisense (guide) strand while the sense (passenger) strand is discarded. Within RISC, the antisense strand mediates gene silencing by guiding the enzymatic machinery to the target mRNA, which is specifically cleaved between positions 10 and 11 opposite to the siRNA antisense strand.[3,4] siRNA-induced gene silencing takes place in the cytoplasm, although evidence for RNAi activity in the nucleus has also been reported.[5−7] The process is catalytic, explaining its outstanding efficacy. In addition, it is based on base-pair recognition, making design of siRNAs easy in theory. siRNAs have thus soon offered great therapeutical promises, but their efficient delivery *in vivo* into target cells and tissues is still a largely unsolved issue.

Nucleic acids and siRNAs in particular do not penetrate animal cells efficiently. To be delivered into the cytosol and elicit RNAi, siRNAs do need assistance to be first internalized by endocytosis and then to be released from the endosomal vesicles. *In vivo*, additional injection route-dependent difficulties arise, such as endothelial wall extravasation, rapid clearance or diffusion throughout tissues.[8]

Vector-based delivery systems, and predominantly complexation with cationic lipids or polymers, provide efficient means to deliver siRNAs into the cell cytoplasm in culture. Many such formulations have also demonstrated some activity in animals,[9,10] and several lipid nanoparticles are under clinical investigation.[11] However, being particles, they generally exhibit limited biodistribution as a consequence of their size.

Direct ligand conjugation to oligonucleotides has been proposed early as an alternative to achieve targeting and intracellular delivery.[12] Being much smaller in size than nanoparticles, conjugated siRNAs are expected to exhibit enhanced tissue diffusion. Many molecules have been used as ligands following various conjugation strategies.[13] Cholesterol−

Received: May 18, 2012
Revised: September 7, 2012
Accepted: October 24, 2012

siRNAs as well as other lipid conjugates have been shown to display enhanced cell uptake and prolonged circulation lifetimes by interacting with serum lipoproteins or albumin.[14,15] Other ligands have been conjugated to bind specifically to surface receptors such as integrins.[16] Still other conjugated ligands were cell-penetrating−peptides (CPPs), i.e., short peptides rich in positively charged amino acids which have been used to enhance cell entry. The conjugation of CPPs to siRNAs has provided contradictory reports, most likely due to contamination by excess free CPP molecules which behave as vectors.[17,18] However, genuine CPP−siRNA conjugates display an overall negative charge and hence enter poorly into cells.[19]

We reported earlier that conjugation of cationic oligophosphospermine to anionic oligonucleotides enhanced their hybridization properties, hence their name ZNA for zip nucleic acids.[20−22] When their net charge is positive, conjugates enter animal cells in culture without carrier.[23] Corey and collaborators also reported carrier-free antisense and antigene activity of single-stranded ZNAs.[24] By annealing a conjugated sense strand to a nonconjugated antisense sequence, we made cationic siRNAs and reported the first evidence of induced gene silencing in animal cells.[23] We meanwhile improved the stepwise synthesis and purification of oligophosphospermine-oligoribonucleotide conjugates which allowed full end characterization of cationic siRNAs. Here we provide further description and a complete study on the activity and the mechanism of action of cationic siRNAs.

EXPERIMENTAL SECTION

siRNA Sequences. All the oligonucleotides were from Eurogentec (Seraing, Belgium). Sense strands were either fully processed by the oligonucleotide supplier or deprotected and purified following the method described below for oligophosphospermine conjugates. Antisense sequences (AS) contained a phosphorothioate linkage as indicated by *. GL3 sense, 5′-CUUACGCUGAGUACUUCGAdTdT-3′; ASGL3, 5′-UCGAAGUACUCAGCGUAAGdT*dT-3′; GL2 sense, 5′-CGUACGCGGAAUACUUCGAdTdT-3′; ASGL2, 5′-UCGAAGUAUUCCGCGUACGdT*dT-3′; Survivin sense, 5′-CCGUCAGUGAAUUCUUGAAdTdT-3′; ASSurvivin, 5′-UUCAAGAAUUCACUGACGGdT*dT-3′.

Oligophosphospermine Conjugated Oligoribonucleotide Synthesis. Oligophosphospermine conjugation was carried out on a K&A synthesizer H8-SE (www.ka-lab.de), using DMT-ON TOM protected oligoribonucleotides provided on CPG solid support by Eurogentec. Oligonucleotide synthesis reagents were from Glen Research. DMT-spermine phosphoramidite was synthesized according to the published procedure.[25] A prolonged coupling time (6 min) was used for phosphospermine coupling. Coupling yields were evaluated by measuring the absorbance at 504 nm of selected recovered DMT fractions diluted in 100 mL of 3% TCA/dichloromethane solution and were 98% in average. After treatment with 20% diethylamine (DEA) in acetonitrile, DMT−OFF conjugates were successively cleaved (1 h) and deprotected (overnight) with methylamine in ethanol/water (EMAM) at 25 °C. After lyophilization, 2′ TOM deprotection was carried out in 500 μL of *tert*-butylammonium fluoride in THF (TBAF) overnight at room temperature, followed by butanol precipitation.

HPLC purifications were carried out using a DIONEX Ultimate 3000, DNAPac-200 column (Dionex), 2.5 mL·min^{-1}; eluent A, NH_4OH 0.1 M, 10% acetonitrile; eluent B, NH_4OH 0.1 M, NaCl 1 M, 10% acetonitrile.

Fractions containing the full length conjugate were pooled, desalted in illustraNAP-25 prepacked columns (GE Healthcare), lyophilized, dissolved in RNase-free water and stored at −20 °C.

MALDI-TOF mass spectra were recorded on a Bruker Daltonics Reflex IV. Matrix used for preparing the samples was saturated with 3-hydropicolinic acid (3-HPA) in a solution 50% acetonitrile/0.05% trifluoroacetic acid (Sigma-Aldrich). Samples were diluted with RNase-free water at about 20 μM, mixed with matrix at sample to matrix ratio of 1:1. MALDI spectra were obtained in positive mode. The parameters used for the mass acquisition were as follows: extraction delay time, 200 ns; laser repetition rate, +19.9 Hz; power of laser, 95%. MALDI spectra were acquired in 100 shot segments that were accumulated until background noise had receded to the best possible level. The mass increase expected per phosphospermine unit is +408 Da.

Characterization by SDS−PAGE and siRNA Formation. Nonconjugated and cationic siRNAs were formed at 20 μM in RNase-free water by mixing an equimolar amount of each sense and antisense strand. Annealing was performed at room temperature for 30 min.

Oligophosphospermine conjugated oligoribonucleotides were analyzed on 12% Tris-glycine SDS−PAGE (stacking gel, 5% acryl-bisacrylamide 19:1/SDS 0.1%; resolving gel, 12% acryl-bisacrylamide 19:1/SDS 0.1%). Samples were loaded in loading buffer (glycerol 5%/SDS 0.1% final); migration buffer was Tris 0.025 M, glycine 0.192 M, SDS 0.1% final.

For duplex analysis, samples were loaded on 10−20% gradient Tris-Tricine precast gels (Biorad), and electrophoresis was carried out in Tris-Tricine 10 mM/0.01% SDS pH 8.3 migration buffer (Biorad).

After electrophoresis, gels were incubated in ethidium bromide (0.5 μg/mL in H_2O) and imaged upon UV transillumination using the G:BOX gel imaging system (Syngene). Quantitative analysis was performed using the dedicated GeneTools software (Syngene).

Cell Culture. A549 cells (human lung carcinoma) stably expressing GL3 luciferase (A549Luc cells) were grown in RPMI medium 1640 (Lonza), supplemented with 10% FBS, 2 mM L-glutamine, 100 units/mL penicillin, 100 μg/mL streptomycin, and 0.8 μg/mL G418. B16-F10 cells (mouse skin melanoma, ATCC CRL-6475) were grown in Dulbecco's modified Eagle's medium containing 4.5 g/L glucose (Eurobio), supplemented with 10% FBS, 2 mM L-glutamine, 100 units/mL penicillin, 100 μg/mL streptomycin.

A549Luc and B16-F10 cells were maintained at 37 °C in a 5% CO_2 humidified atmosphere.

Cationic siRNA Incubation and Transfection Experiments. The day before the experiment, 2.5 × 10^4 cells were seeded in 24-well tissue culture plates in 1 mL of fresh complete medium containing 10% FBS. Before the incubation with cationic siRNAs, the medium was either replaced by 0.5 mL of fresh serum-free medium or 0.5 mL of complete medium. For a triplicate experiment, cationic siRNAs were diluted in 300 μL of Opti-MEM (Life Technologies), and the solutions were vortex-mixed for 10 s and immediately added to the cells (100 μL per well). Plates were hand-rotated to ensure homogeneity and incubated at 37 °C. After 4 h incubation, the medium was completed to 1 mL of complete medium containing 10% FBS. The plate was further incubated at 37

°C for 24 or 48 h. As transfected controls, standard siRNA lipoplexes were formed using the cationic lipid reagent INTERFERin (Polyplus-transfection SA) as described by the supplier.

Luciferase Activity and Total Protein Assay. The cells were rinsed with 1 mL of PBS and then were lysed with 100 μL per well of cell culture lysis buffer 1× (Promega) at room temperature for 30 min. The lysates were collected and centrifuged at 15000*g* for 5 min at 4 °C. Luciferase enzyme activity was quantified with a Centro LB960 luminometer (Berthold) with 2.5 μL of supernatant lysate and after addition of 50 μL of luciferin solution (Promega). The protein concentration was measured by the BCA protein assay kit (Pierce). The luciferase activity was expressed as relative light units integrated for 10 s (RLU) per well or RLU per mg of cell protein (RLU/mg). The luciferase silencing efficiency was calculated relative to the luciferase activity of nontreated A549Luc cells.

Cell Uptake Assessment. Fluorescently labeled standard GL3 siRNA or cationic GL3 siRNAs were obtained by annealing nonconjugated or conjugated sense strand with a 3′-Rhodamine GL3 antisense strand (Eurogentec). A549Luc cells were incubated with fluorescent cationic siRNAs or transfected with fluorescent standard siRNA lipoplexes as described above.

Microscopic Observation. Cells were observed in PBS by fluorescent microscopy (Nikon Eclipse TE2000-S fluorescent microscope coupled to a Nikon digital camera).

Flow Cytometry. A549Luc cells incubated with fluorescent cationic siRNAs were washed, submitted to trypsin treatment and resuspended in complete medium. The cell suspensions were counted with an automated cell counter (Biorad) to verify the concentration (<500 cells/μL). Fluorescent data were gathered using a microcapillary flow cytometer Guava EASY-CYTE 6HT (Guava Technologies, Millipore) equipped with a 488 nm diode laser. Rhodamine fluorescence was collected at 583 nm. Data were analyzed using GuavaSoft (Millipore). Forward scatter gating was set to exclude dead cells and debris. A minimum of 1000 events were collected to each histogram. Analytical gates were chosen such that <2% of control cells fell within the positive region. The *X*-mean value expressing the mean intensity of fluorescence per fluorescent cell was plotted as a function of percentage of serum in the cell culture medium.

siRNA Degradation Assays. 1.5 μg of conjugated and nonconjugated siRNAs was incubated in 6 μL of 10% FBS at 37 °C for 0, 2 and 4 h. When indicated, 4 U of pancreatic ribonuclease inhibitor RNaseOUT (Life Technologies) was added prior to FBS.[26]

Alternatively, 50 pmol of conjugated and nonconjugated siRNA was incubated in the presence of 0, 1, 10 or 100 ng of RNase A (Qiagen) in 10 μL of H_2O at 37 °C for 2 h.

After incubation, samples were analyzed on Tris-Tricine SDS−PAGE as described above.

Total RNA Extraction for RT-qPCR or 5′RACE Assays. Total RNA from triplicate experiments was isolated from treated or nontreated A549Luc or B16-F10 cells using RNA NOW reagent (Biogentex) following the manufacturer's instruction. After isopropanol precipitation, RNA was resuspended in RNase-free water and stored at −80 °C. RNA quality was assessed by agarose gel electrophoresis and A260/280 ratio.

RNAi Specific Cleavage Determination Using 5′RACE Assays. 5′RACE was carried out using the Gene Racer kit (Life Technologies). 1 μg of extracted RNA was ligated with 25 ng of Gene Racer oligonucleotide in a final reaction containing T4 RNA ligase (5 U), 1× ligase buffer, 1 mM ATP and 40 U of RNaseOUT and incubated at 37 °C for 1 h. After ethanol precipitation, ligated RNA was washed and resuspended in RNase-free water. For cDNA synthesis, 5 μL of ligated RNA, 500 μM dNTPs and 200 nM GL3-specific RT primer (5′-CGTGATGGAATGGAACAAC-3′) were incubated in a 10 μL volume at 65 °C for 5 min to denature the RNA and then chilled on ice for at least 1 min. A mix containing 1× first strand buffer, 5 mM dithiothreitol (DTT), 200 U of Superscript III Reverse transcriptase and 40 U RNaseOUT was added to RNA/primer mix to a final volume of 20 μL. The reaction was performed at 55 °C for 45 min, heat inactivated at 70 °C for 15 min and then chilled on ice. 2 U of RNase H was added in each tube and then incubated at 37 °C for 20 min.

Subsequent PCR reactions were performed in a final volume of 20 μL in iCycler thermocycler (Biorad). The final reaction mixtures were composed of 2 μL of the reverse transcription reaction, 1 U of EconoTaq DNA Polymerase (Lucigen), 1× EconoTaq buffer, 200 μM dNTP, 3 mM $MgCl_2$ and 200 nM concentrations of each of the PCR primers (gene racer 5′ primer, 5′-CGACTGGAGCACGAGGACACTGA-3′; GL3 reverse primer, 5′-ACGGTAGGCTGCGAAATGCCCAT-3′). Cycling conditions were 10 cycles (94 °C for 20 s, 67 °C for 20 s, 72 °C for 15 s) and 25 cycles (94 °C for 20 s, 64 °C for 20 s, 72 °C for 15 s). PCR reactions were analyzed on 3% Seakem agarose gel (Lonza).

Quantification of the Survivin mRNA Using RT-qPCR. cDNA was prepared as follows: 1 μg of total RNA, 500 μM dNTPs, 2.5 μM oligodT and 100 nM Survivin RT primer (5′-GCCACAAAACCAAAGAGAGG-3′) were incubated in a 10 μL volume at 65 °C for 5 min to denature the RNA and then chilled on ice for at least 1 min. Mix containing 1× first strand buffer (Life Technologies), 5 mM DTT, 5 mM $MgCl_2$, SuperScript III RT (200 U) and RNase OUT (40 U) was added to RNA/primer mix to a final volume of 20 μL. The reaction was performed at 50 °C for 50 min, heat inactivated at 85 °C for 5 min and then chilled on ice. Samples were incubated with RNase H (2 U) at 37 °C for 20 min.

All subsequent qPCR reactions were performed in duplicate in a final volume of 10 μL using a Rotor-Gene 6000 instrument (Corbett Life Science). Reaction mixtures were composed of 5 μL of Sensimix NoRef (Quantace), 3 mM $MgCl_2$, 10 ng to 10 pg of cDNA. Survivin target was amplified using a SYBR Green-based qPCR assays with a 200 nM concentration of each primer (Survivin forward, 5′-TCTGGCAGCTGTACCTCAA-GAACT-3′; Survivin reverse, 5′-AAACACTGGGCCAAAT-CAGGCT-3′). Cycling conditions were 95 °C for 15 s, 63 °C for 20 s, 72 °C for 15 s. HPRT1 mRNA was used for normalization and was quantified using a probe-based detection reaction, with a 600 nM concentration of each primer (HPRT1F, 5′-TGGTTAAGCAGTACAGCCCCA-3′; HPRT1R, 5′-GGCCTGTATCCAACACTTCGAGA-3′) and 300 nM of the ZNA-modified hydrolysis probe (FAM-CACCAGCAAGCTTGC-Z_4-BHQ_1, Metabion International AG) (see supplementary table in the Supporting Information for Survivin and HPRT1 sequence location). Cycling conditions were 95 °C for 15 s and 60 °C for 1 min. The presence of PCR inhibitors in samples has been assessed by determining the qPCR efficiency (*E*) for both targets in each sample using the dilution method. HPRT1 was used as reference gene since its expression compared in control and treated samples was shown to be stable (7 samples; cDNA

corresponding to 10 ng of total RNA; mean C_q = 21.1; SD = 0.214). The relative expression of the survivin mRNA was calculated using the $\Delta\Delta C_q$ method following the relation

$$\text{relative survivin mRNA expression} = (1 + E_{\text{survivin}})^{\Delta Cq\text{survivin(control}-\text{sample)}} / (1 + E_{\text{HPRT1}})^{\Delta Cq\text{HPRT1(control}-\text{sample)}}$$

Survivin Protein Expression Level by Western Blot. B16-F10 cells in a 24-well plate were rinsed with 1 mL of ice-cold PBS and scraped off the dish in 30 μL per well of RIPA buffer containing 50 mM Tris-HCl, 150 mM NaCl, 5 mM EDTA, 0.5% Triton, 0.05% SDS and protease inhibitor cocktail (Sigma-Aldrich). The lysates were incubated on ice for 20 min and then centrifuged at 15000*g* for 5 min at 4 °C. 40 μg of total protein lysate was denatured in Laemmli buffer with β-mercaptoethanol at 95 °C for 5 min prior to being run on 15% SDS–PAGE. The gel was transferred on a PVDF membrane (Millipore). For Survivin protein immunodetection, all the incubations and washing steps were done in PBS/Tween20 0.1%/BSA 5%: blocking for 1 h at room temperature, incubation with the rabbit anti-survivin polyclonal antibody (Cell Signaling Technology, #2808 rabbit) diluted in 1/1000 overnight at 4 °C, then incubation at room temperature for 1 h with a goat peroxidase-conjugated anti-rabbit IgG (AP132P, Millipore) diluted at 1/10000. For GAPDH detection, all the incubations and washing steps were performed in PBS/Tween20 0.1%/nonfat dry milk 5%: blocking for 1 h at room temperature, incubation with a mouse anti-GAPDH monoclonal antibody (Ambion, Austin, TX) diluted at 1/8000 overnight at 4 °C, then incubation at room temperature for 1 h with a goat peroxidase-conjugated anti-mouse IgG (A9917, Sigma-Aldrich) diluted at 1/20000. Signal revelation was done using the SuperSignal West Pico Chemiluminescent Substrate (Pierce) following manufacturer's instructions using darkroom development techniques. Kodak films were then imaged with the G:BOX imaging system (Syngene). Survivin and GAPDH immunoblotting were carried out successively, without stripping step.

RESULTS

Synthesis, Deprotection and Purification of Phosphospermine–Oligoribonucleotide Conjugates. In the present work, we used the standard siRNA design consisting of two annealed strands of 19 ribonucleotides, each extended with an overhanging dTdT at its 3′ end as described originally by Tuschl and collaborators[1] (Figure 1). A phosphorothioate linkage between the 2 dTs was the only modification of the antisense strand. We focused our initial efforts on the synthesis of the phosphospermine-conjugated sense strand which is produced by stepwise conjugation of 20 to 35 phosphospermine units at the 5′ end of the oligoribonucleotide following standard solid state phosphoramidite chemistry.[22,25] Due to the iterative nature of the process, the amount of full length product recovered is primarily conditioned by a good coupling yield of the phosphospermine at each cycle. We achieved a coupling yield of 98%, meaning that elongation stopped for 2% of the molecules at each cycle, resulting in a polydisperse crude material. Purity therefore depends on the ability to resolve polydispersity. In our first study, DMT-ON full length products were simply enriched using reverse phase RP cartridges[23] and a more efficient purification step was required. Anion exchange

a.

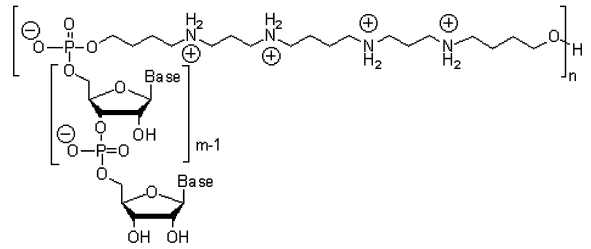

b.

$^{5'}$ UCGAAGUACUCAGCGUAAGdT*dT $_{3'}$

$_{3'}$ dTdTAGCUUCAUGAGUCGCAUUC–Z_n $^{5'}$

Figure 1. Structure of 5′- conjugated oligoribonucleotide (a) and cationic siRNA containing *n* phosphospermine units (b). * represents a phosphorothioate linkage.

IEX-HPLC purification had been successfully developed for oligodeoxyribonucleotides containing few phosphospermines.[25] It was conducted under highly basic conditions in order to deprotonate spermine residues. Surprisingly such basic conditions did not induce RNA hydrolysis, and we therefore applied this purification method to our deprotected RNA conjugates (Figure 2a). Careful fractionation and pooling allowed recovery of full length product, which was desalted, lyophilized and resuspended in H_2O. No solubility issues were observed during the process in spite of the macrozwitterionic nature of the compounds.

Characterization of the Phosphospermine–Oligoribonucleotide Conjugates. In addition to IEX-HPLC analysis (Figure 2b), an alternative method for assessing the purity of the final product was implemented. Denaturating polyacrylamide gel electrophoresis (D-PAGE) is a powerful method for resolving mixtures of essentially linear biomolecules according to their length. Unfortunately, the net charge of the conjugates was too small for the electric field to drive the molecules through the gel in denaturating urea conditions used for nucleic acids D-PAGE. Moreover, we also experienced that conjugates tend to stick on glass plates. Protein D-PAGE is based on sodium dodecyl sulfate (SDS) detergent solubilization of the denaturated linear protein and its migration as anionic SDS micelles.[27] We hypothesized that the SDS/hydrophobic amino acid interaction could be replaced by an anionic SDS/cationic spermine interaction and hence allow us to resolve oligospermine-oligonucleotides according to their length. Figure 2c shows that SDS–PAGE was indeed able to resolve the conjugates at the phosphospermine level. Moreover, the presence of SDS in the loading buffer avoided conjugates' sticking on the glass plate before entering into the gel. Since conjugates were detected postelectrophoretically using ethidium bromide staining, we next asked whether this method was quantitative and able to assess the level of purity with respect to the number of phosphospermines. Increasing amounts of Z_{25}- and Z_{30}-RNA conjugates were loaded on a SDS–PAGE gel and stained with ethidium bromide after electrophoresis (Figure 3a). While the Z_{25}-conjugate appeared as a single band, the Z_{30}-conjugate showed, besides a major band, a significant amount of impurities (Z_{n-1}-conjugates) as revealed by discrete bands migrating as a phosphospermine ladder. Fluorescence inten-

dx.doi.org/10.1021/mp300278b | *Mol. Pharmaceutics* XXXX, XXX, XXX–XXX

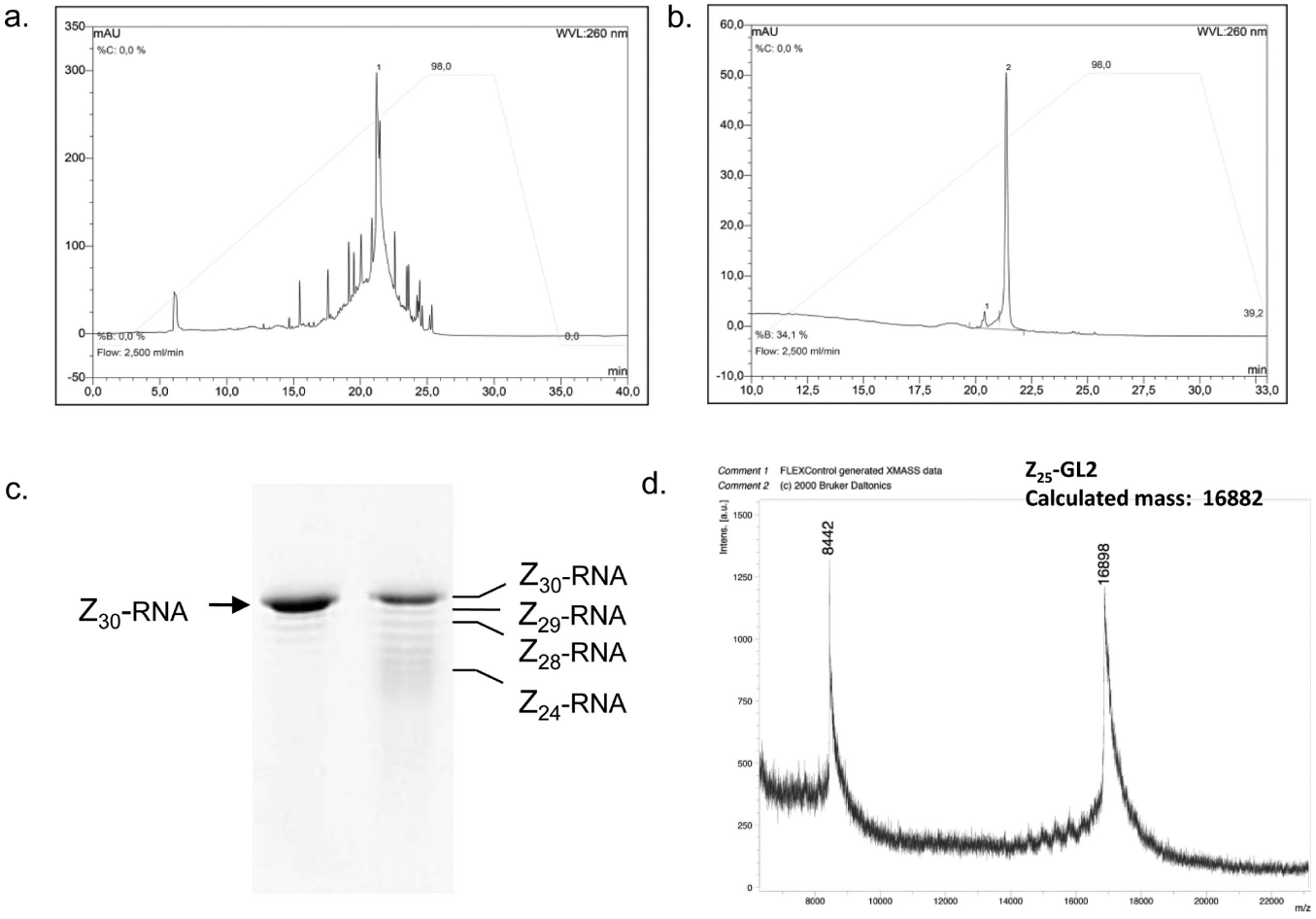

Figure 2. Purification and characterization of oligophosphospermine−oligoribonucleotide conjugates (Z_n-RNA) (see Experimental Section). Crude conjugates are typically purified using basic IEX-HPLC (a). Selected fractions are pooled and analyzed using the same HPLC procedure (b). Two fractions are analyzed using SDS−PAGE (c). Identity is achieved using MALDI-TOF mass spectrometry (d).

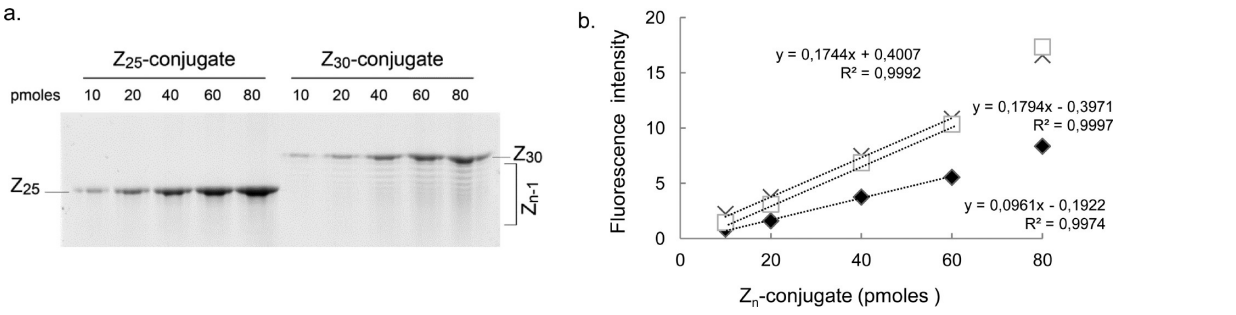

Figure 3. Purity assessment. Increasing quantities of Z_{25}- and Z_{30}-conjugates were analyzed using SDS−PAGE followed by ethidium bromide staining (a). Fluorescence intensities of discrete bands corresponding respectively to Z_{25}-conjugate (cross) and Z_{30}-conjugate (black rhombs) as well as cumulated intensities of Z_{30}-conjugate and truncates (squares) quantified using GeneTools software (Syngene) were plotted as a function of loaded quantities (b) .

sities of full length products as well as the cumulated intensities of Z_{30}-conjugated species present in each track were quantified using dedicated software (GeneTools, Syngene). In all cases, the fluorescence increased linearly with the amount of loaded material (Figure 3b). As expected, the integrated fluorescence intensity of the Z_{25}-conjugate and the total fluorescence intensities in the Z_{30}-conjugate lane were similar, showing a good correlation between oligonucleotide amount (based on optic density measurement) and ethidium bromide fluorescence, irrespective of the number of phosphospermines. The full length over total intensities ratio showed that Z_{30} accounted for 55% of the conjugates present in the sample.

All batches were analyzed by SDS−PAGE, and only conjugates with at least 80% full length purity were used for subsequent experiments. With such a specification, we routinely recovered 15 nmol from a 0.5 μmol scale oligonucleotide synthesis.

As a final control, conjugate molecular weights were assessed using MALDI-TOF mass spectrometry (Figure 2d). Due to the high molecular weight of the conjugates (approximating 19 kDa) and their high propensity to form multiple salt adducts,

dx.doi.org/10.1021/mp300278b | *Mol. Pharmaceutics* XXXX, XXX, XXX−XXX

mass spectra could not be a means to assess complete deprotection and/or the oligonucleotide sequence. However, spectra provided the confirmation of the number of phosphospermines (±408 Da per unit), since the difference between experimental and calculated mass varied from +16 to +150 Da.

Formation of Conjugated siRNA and Carrier-Free Delivery. Cationic siRNAs consist of an oligophosphospermine-conjugated RNA sense strand annealed with a standard antisense oligoribonucleotide. Together as a duplex, they are expected to be substrate of the RISC machinery like any other siRNA. Assembling both strands is also critical to combine functions carried out by each entity separately: the conjugate is the carrier of the antisense strand which mediates gene silencing. We thus worked at gaining further insight into conjugated duplex formation.

Cationic siRNAs were formed at room temperature in RNase-free water, by mixing the conjugated sense strand and the complementary antisense sequence in equimolar quantities. Annealing was monitored on gradient SDS–PAGE, allowing visualization of both strands. As shown in Figure 4a, when both strands are mixed, neither the conjugate nor the antisense strand can be seen, but a novel entity with reduced electrophoresis mobility appears. Interestingly, when the phosphospermine-conjugated sense strand is mixed with an unrelated sequence lacking complementarity (Figure 4b), both strands keep migrating separately in the gel, and no retarded band corresponding to a complex is observed. Taken together, these data demonstrate that the retarded band observed when both strands are complementary is the duplex.

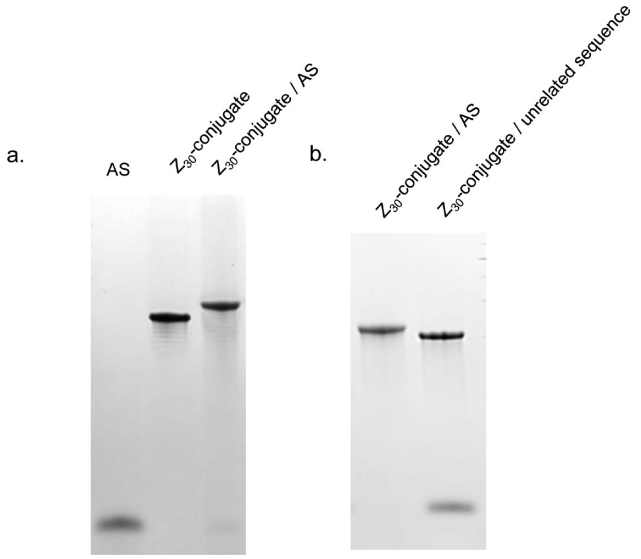

Figure 4. Cationic siRNA formation. Single-stranded Z_{30}-conjugate was mixed with the antisense strand (AS) in equimolar amount and duplex formation was observed by an electrophoretic migration shift on SDS–PAGE (SDS–Tris-Tricine 10–20%) (a). Duplex formation occurred when Z_{30}-conjugate was mixed together with its complementary AS sequence (Z_{30}/AS) while no annealing was observed when the sequences were not complementary (Z_{30}/unrelated sequence) (b).

Mixing positively and negatively charged molecules can generate coprecipitates. In the case of the related complex formation between polynucleotides and the cationic polymer polyethylenimine, the key parameter is the amine over phosphate molar ratio (N/P ratio) which determines the particle charge, size and cellular delivery properties. To rule out precipitation during the annealing step, we mixed the Z_{25}- and Z_{30}-conjugates with varying amounts of their antisense strands and performed SDS–PAGE (data not shown). While the duplex was completely formed when the strand ratio was 1/1, above and below this ratio the strand in excess remained as a single strand. Precipitation was only observed when the antisense strand was 1.5-fold in excess to the Z_{25}-conjugate, or 2-fold in excess to the Z_{30}-conjugate. For the Z_{20}-conjugate, precipitation occurred when mixed with the antisense strand close to the 1:1 ratio required for siRNA formation. Interestingly, these results showed that precipitation occurred when the N/P ratio was close to 4/3.

In summary, truly cationic siRNAs are formed with $Z > 20$ for an equimolar amount of the antisense strand. No precipitation was observed unless the antisense strand was added in excess. Moreover, Watson–Crick recognition between a phosphospermine-conjugated RNA and its complementary strand is maintained despite additional stability brought about by the high number of positive charges.[21]

We next used a 3′-fluorescently labeled antisense strand to monitor cell penetration of siRNA by direct microscopic observation. When the siRNA lacking spermines was delivered with a cationic lipid, the fluorescent signal appeared mainly distributed as a few rather large spots within the cell (Figure 5a), presumably endocytotic vesicles.[28] When incubated with annealed Z_{25}-conjugated siRNA, every cell exhibited an intracellular fluorescence (Figure 5b). Although some diffuse signal could be observed in some cells, the conjugated siRNA appeared essentially distributed following a punctate pattern, the high number of spots throughout the cytosol demonstrating an efficient cell entry. We also made the important observation that a Z_{30}-conjugated oligonucleotide unable to anneal with the antisense strand due to the lack of sequence complementarity (Figure 5b) was unable to deliver the antisense strand into cells (Figure 5c). Moreover, no intracellular fluorescence was observed when the strands were complementary, but the antisense strand in excess induced precipitation at the annealing step. Taken together, these results show that cationic siRNAs are able to enter cells in the absence of any carrier. Cell penetration requires complementary RNA strands properly annealed in a 1 to 1 ratio. This strongly suggests that they interact not with the cell membrane as preexisting particles formed upon electrostatic interactions but, instead, as non-aggregated molecules. In the cell, they exhibit a vesicular pattern which is in favor of an endocytotic cell uptake mechanism.

Relationship between Uptake, Activity and the Number of Phosphospermines. As a preliminary proof-of-principle of self-delivery using cationic siRNAs, we previously reported that a Z_{30}-conjugated siRNA was able to specifically knock down luciferase expression in A549Luc cells in the absence of serum, while the Z_{20}-conjugated siRNA had no effect.[23] To further investigate the impact of overall charge on conjugated-siRNA activity, A549Luc cells were incubated with 100 nM luciferase targeting cationic siRNAs containing either 20, 25, 30 or 35 phosphospermines (Figure 6a). In the absence of serum in the culture medium for the first 4 h of incubation, 95% silencing was achieved with Z_{25}, Z_{30} and Z_{35} species, a value similar to that obtained with 10 nM standard siRNA formulated with a commercially available cationic lipid transfection reagent. Nonconjugated siRNA alone at the concentration 100 nM had no activity. It is noteworthy that

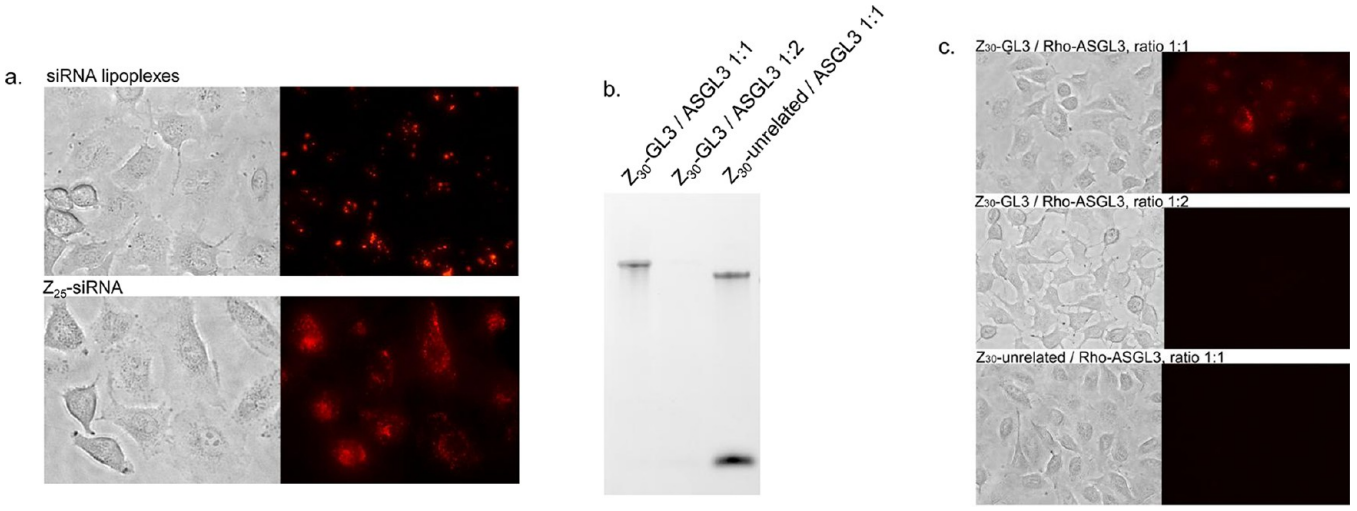

Figure 5. Cationic siRNAs enter cells in the absence of transfection reagent. (a) Observation of A549Luc cells incubated for 24 h in the presence of serum with Rhodamine-siRNA (10 nM) delivered with the cationic lipid transfection reagent INTERFERin (upper panel), or Rhodamine-Z_{25}-cationic siRNA (100 nM) (lower panel). (b) Rhodamine labeled GL3 antisense strand (ASGL3) was mixed with sense strand Z_{30}-GL3 (molar ratio 1:1 and 2:1) or with Z_{30}-unrelated sequence (molar ratio 1:1). Samples were monitored for duplex formation by SDS−PAGE (Tris-Tricine 10−20%), and (c) used for incubation with A549Luc cells (100 nM). Cells were observed 24 h postincubation.

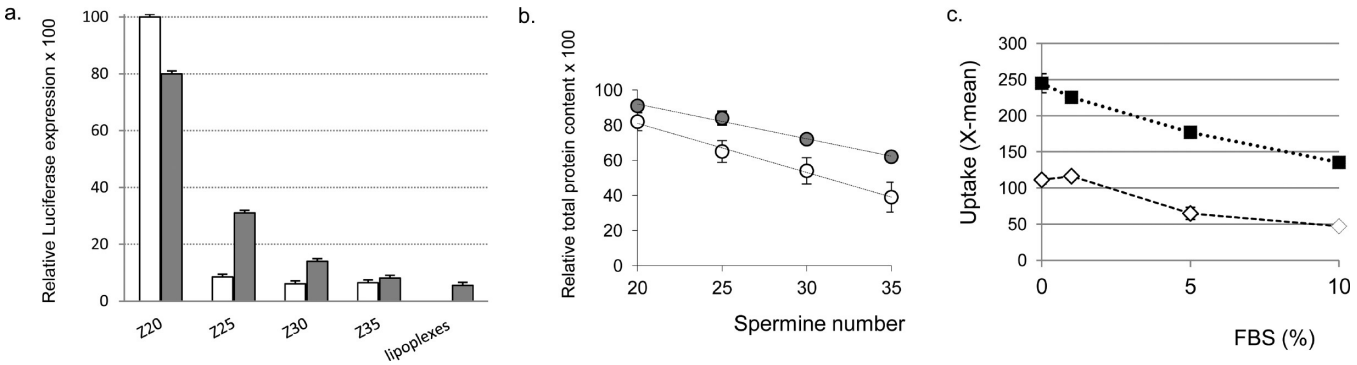

Figure 6. Phosphospermine number and serum impact. (a, b) A549Luc cells were incubated with 100 nM of cationic siRNAs GL3 targeting the luciferase gene and carrying 20 to 35 phosphospermine moieties, in the absence of serum for 4 h (white bars or circles) or in serum containing medium (gray bars or circles). As a positive control, cells were transfected with 10 nM lipoplexes (GL3/INTERFERin). 48 h postincubation, cells were analyzed for luciferase activity (a) and total protein content (b). Data are expressed as the percentage of luminescence unit (RLU) relative to untreated cells (a) or percentage of total protein content relative to untreated cells (b). Each point is the mean of three samples ± SD. (c) A549Luc cells were incubated with 100 nM fluorescently labeled cationic siRNAs, carrying 25 (white rhombs) and 30 (black squares) phosphospermine moieties in the presence of increasing amount of fetal bovine serum in the cell culture medium. 24 h postincubation, uptake was examined by flow cytometry. Data are expressed as the mean fluorescence intensity per cell (*X*-mean), and each point is the mean of three samples ± SD.

the improved conjugate synthesis and purification procedure led to a significant decrease in effective concentration (by a factor of 5), since Z_{30}-siRNA was previously reported to require a 500 nM concentration to display a similar activity.[23] However, despite purification, Z_{20}-siRNA was inefficient at this concentration, as previously observed.

In the presence of serum, we surprisingly discovered that cationic siRNA with a natural ribonucleotide backbone remained active. Though silencing was slightly reduced for Z_{25}-conjugated siRNA, serum perturbation disappeared upon increasing the number of phosphospermine units to 30 and 35.

In parallel to activity, a charge-dependent decrease in total protein content per well was also observed, which may be attributed to cell toxicity (Figure 6b). Interestingly, serum appeared to have a protective effect.

We next asked whether the charge-dependent activity could be the consequence of differential cell uptake efficiencies. To this end, A549Luc cells were incubated with fluorescently labeled Z_{25}- or Z_{30}-conjugated siRNAs, in the absence or presence of an increasing percentage of fetal bovine serum in the culture medium. Intracellular fluorescence was monitored by flow cytometry 24 h postincubation (Figure 6c). We first found that all cells exhibited a fluorescent signal, confirming that cationic siRNAs were taken up by 100% cells. The amount of Z_{30}-conjugated siRNAs per cell, expressed as the median fluorescence intensity per cell (*x*-mean value), was higher than for its Z_{25} counterpart. The same observation was made when comparing Z_{35}- and Z_{30}-conjugated siRNAs (data not shown), indicating that the level of uptake is actually modulated by the number of phosphospermine units, with the more cationic the siRNA, the more efficiently it enters cells. Intracellular levels of both Z_{25}- and Z_{30}-conjugated siRNAs were decreasing with serum concentration increase, achieving 50% and 40% reduction at 10% FBS, respectively. It is thus likely that reduced uptake is the major reason for the slight decrease in

dx.doi.org/10.1021/mp300278b | *Mol. Pharmaceutics* XXXX, XXX, XXX−XXX

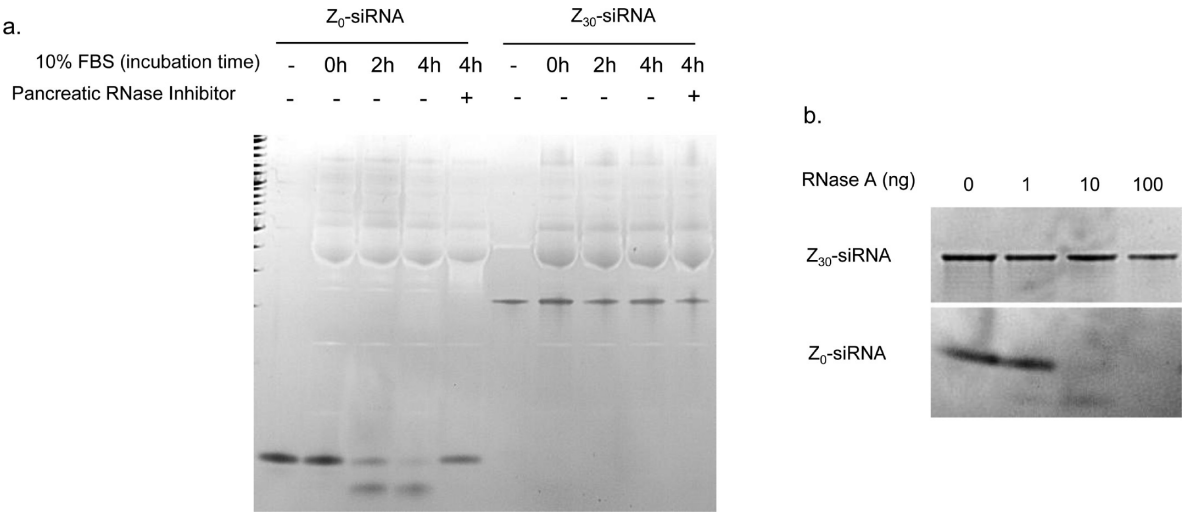

Figure 7. Z_{30}-conjugated siRNA is not degraded by serum components and pancreatic ribonucleases. 1.5 μg of nonconjugated Z_0-siRNA or Z_{30}-siRNA was incubated in 6 μL of FBS 10% at 37 °C, in the absence or in the presence of pancreatic ribonuclease inhibitor (a). 50 pmol of Z_0-siRNA or Z_{30}-siRNA was incubated in the presence of 0, 1, 10 or 100 ng of RNase A for 2 h at 37 °C (b). Samples were analyzed on SDS−Tris-Tricine polyacrylamide 10−20% gel followed by ethidium bromide staining.

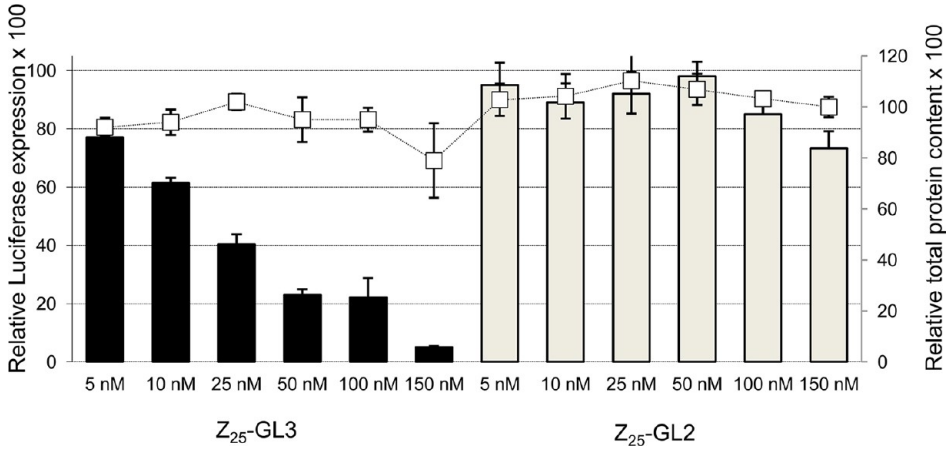

Figure 8. Cationic siRNAs induce specific and dose-responsive gene silencing. A549Luc cells were incubated in the presence of serum with increasing amount of Z_{25} cationic siRNAs targeting the luciferase GL3 gene (Z_{25}-GL3) or the negative control Z_{25}-GL2 displaying 3 mismatches with the luciferase GL3 sequence. 48 h postincubation, cells were analyzed for luciferase activity and total protein content as described in the Experimental Section. Data are expressed as the percentage of luminescence unit (RLU)/μg of protein relative to untreated cells (left *Y*-axis, bars) or percentage of total protein content relative to untreated cells (squares). Each point is the mean of three samples ± SD in a representative experiment.

activity observed when cells were incubated in the presence of serum.

Stability of Cationic siRNAs in Serum. RNase A-like activities have been shown to lead to fast siRNA degradation in blood serum.[26,29] The observation that cationic siRNAs remained active in serum conditions suggests that the molecules were not extensively degraded prior to being taken up by the cells. To examine their resistance toward nuclease hydrolysis, a conjugated Z_{30}-siRNA and its nonconjugated counterpart were incubated in 10% fetal bovine serum and analyzed over time using SDS−PAGE (Figure 7a). We confirmed that the control siRNA was degraded within 4 h incubation in serum, and that degradation was prevented by addition of a RNase A inhibitor. Under the same conditions, Z_{30}-conjugated siRNA remained unaffected. Similar experiments were performed with lower homologues containing 5 and 10 phosphospermines, and although some degradation was observed, robust stabilization was still observed (data not shown). We further conducted degradation assays using increasing amounts of purified bovine RNase A (Figure 7b). Again, Z_{30}-siRNA remained intact while the nonconjugated control was completely digested.

These data demonstrate that an oligophosphospermine tail prevents the siRNA moiety from serum-induced degradation. This finding confirms that the slight decrease in uptake that was observed upon addition of serum was not due to degradation. Instead, it might argue for an interaction between cationic siRNAs and serum components, which would interfere with or compete for binding to membranes and subsequent internalization. As a negatively charged carrier protein and major serum component, albumin is an obvious candidate.

Silencing Specificity and RISC Signature. We examined the mechanism by which cationic siRNAs suppress gene expression. To address the question of specificity, A549Luc cells were incubated in the presence of serum with various amounts of Z_{25}-siRNA targeting the expressed GL3 luciferase

dx.doi.org/10.1021/mp300278b | *Mol. Pharmaceutics* XXXX, XXX, XXX−XXX

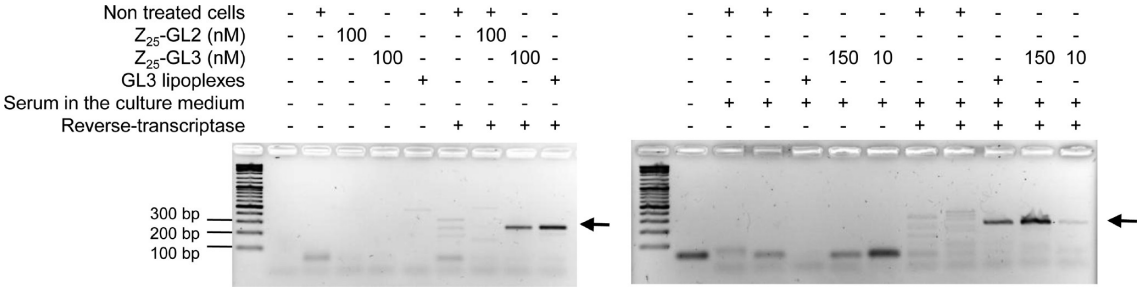

Figure 9. Cationic siRNAs mediate gene silencing through RNA interference mechanism. A549Luc was incubated in the presence or in the absence of serum for 4 h with Z_{25}-GL3 targeting the luciferase gene or Z_{25}-GL2 mismatch or transfected with standard GL3 siRNA/INTERFERin lipoplexes. Total RNA was extracted 48 h post-treatment, and submitted to 5′RACE assays as described in the Experimental Section. PCR reactions were analyzed on 3% agarose gel to visualize the 255 bp RNA-induced silencing complex RISC-mediated cleavage product (arrow).

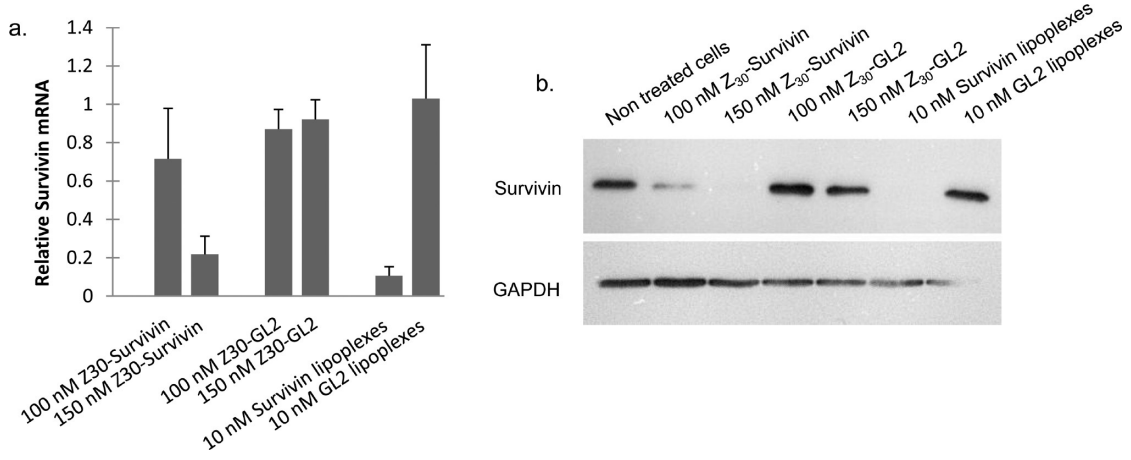

Figure 10. Survivin transcript and protein are significantly decreased upon incubation with survivin targeting cationic siRNAs in B16-F10 melanoma cell. B16-F10 cells were incubated in the presence of serum with Z_{30}-survivin, Z_{30}-GL2 control or nonconjugated siRNA/INTERFERin particles. Survivin mRNA was quantified by RT-qPCR 18 h postincubation using HPRT1 as reference gene for normalization. Bars are the expression relative to untreated samples and represent the mean of three independent experiments. SD are indicated (a). Survivin protein was detected in cellular extracts prepared 48 h postincubation. GAPDH was used as loading control (b).

gene (Z_{25}-GL3) or with another luciferase sequence presenting three mismatches (Z_{25}-GL2). As shown in Figure 8, Z_{25}-GL3 displayed dose-responsive gene silencing with IC50 value in the range of 25 nM without toxicity, whereas Z_{25}-GL2 had no effect on the cells.

Next, it was crucial to investigate whether the specific gene silencing occurred through an RNAi mechanism. Indeed, the long phosphospermine tail at the 5′ end of the sense strand might impede RISC binding or activity. We thus carried out rapid amplification of cDNA ends (5′RACE) analysis as previously used by others to demonstrate the specific cleavage of the target mRNA.[14] Cells treated with Z_{25}-GL3, or with Z_{25}-GL2 or GL3 standard siRNA vectorized with a cationic lipid as controls, were analyzed 48 h post-treatment. As depicted in Figure 9, a PCR product of the expected size (255 bp) was found in samples incubated with Z_{25}-GL3 in the absence or in the presence of serum, as well as in cells transfected with standard siRNA GL3/cationic lipid complexes. The sequencing of the amplicons confirmed the cleavage of the target at the expected site (Supplementary Figure 1 in the Supporting Information). Strikingly, the RNAi signature was even present in the sample from cells incubated with 10 nM Z_{25}-GL3 in the presence of serum. No specific cleavage product was detected from samples treated with Z_{25}-GL2.

Knockdown of a Cellular Gene. To examine the cationic siRNA activity in a more relevant cellular model, we targeted the survivin gene in B16F-10 murine melanoma cells. Survivin is a member of the inhibitor of apoptosis protein (IAP) family which plays a role in suppression of apoptosis, regulation of cell division and cell motility. It is overexpressed in numerous human cancers, and as such, it is a prominent anticancer target.[30−32]

B16-F10 cells were incubated with Z_{30}-survivin cationic siRNA in the presence of serum, and we analyzed the activity at both the transcript and protein levels. As shown in Figure 10a, the Z_{30}-conjugated survivin siRNA led to a 28% and 78% reduction of survivin mRNA, at 100 nM and 150 nM, respectively. In comparison, the same concentrations of control Z_{30}-GL2 conjugated siRNA had no effect. Survivin mRNA knockdown persisted 48 h postincubation (data not shown), inducing a drastic decrease in protein level (Figure 10b).

Finally, to assess the activity of a cationic siRNA at the cellular level, we targeted the nuclear envelope protein LaminA/C in HeLa cells, using a Z_{25}-conjugated siRNA.[1] The protein was detected by immunocytochemistry using a specific LaminA/C antibody. In agreement with the observation that conjugated siRNAs were able to enter into all plated cells, LaminA/C expression was reduced in the entire cell population incubated with the target cationic siRNA (Supplementary Figure 2 in the Supporting Information).

Together with the data described above, this result showing that efficient cationic siRNAs mediated gene silencing in a third

mammalian cell line, and on a third target gene, provides the general demonstration that oligophosphospermine conjugated siRNAs trigger the inhibition of gene expression, in a carrier-free manner.

DISCUSSION

Following our earlier finding that cationic siRNAs were able to mediate carrier-free gene silencing in animal cells, we here concentrated our efforts toward improving the synthesis and characterization of the conjugates. We then explored in detail their activity and the mechanism by which they mediate gene expression inhibition.

Conceptually, a cationic siRNA bears an overall positive charge in order to favor binding and clustering of cell-surface syndecans and trigger endocytosis.[9] As a potential drug, it must also remain as a molecule in solution to benefit from intratissue diffusion properties more favorable than those of nanoparticles. However, playing with charge may induce aggregation that could end up with solubility issues. In this respect, there are two critical steps in the formation of a soluble cationic siRNA: the synthesis of the highly cationic conjugated sense strand and the annealing step which brings about novel anionic charges carried by the antisense strand.

The oligophosphospermine−oligonucleotide conjugates were synthesized stepwise on solid supports following the phosphoramidite chemistry. This process allowed straightforward variation of the global charge which was the key parameter supposed to modulate both physical and biological properties of the conjugates. According to the phosphoramidite chemistry developed, the interspermine phosphodiester linkages introduced a negative charge for every spermine block, thus providing three potential positive charges per spermine unit. Consisting of an iterative process, stepwise synthesis reduced the overall yield and required large excess amounts of the polyamine synthon at each step. Facing this problem, we have increased the phosphoramidite spermine coupling yield to 98%. However, a polydisperse crude material was generated. IEX-HPLC purification was then developed, and even if the resolution could be further improved, fractions containing >80% full length product could be obtained. Importantly, while direct conjugation of oppositely charged polymers in solution is known to represent a challenge in terms of solubility, our synthetic route also provided soluble conjugates.

Duplex formation could compromise solubility, since novel neutralizing charges are provided by the antisense strand. This has been observed previously for conjugates containing highly cationic peptides.[19] With the exception of the Z_{20}-conjugate, we found that mixing the conjugated strand with its complementary sequence in equimolar quantities allowed duplexes to form and remain soluble in water. Interestingly, precipitation did occur for a given excess of the antisense strand that depended on the number of phosphospermine units of the sense strand: 2-fold and 1.5-fold excess for Z_{30}- and Z_{25}-conjugates, respectively. For the Z_{20}-conjugate, precipitation already occurred during duplex formation, i.e., at a molar ratio 1:1. In all cases mentioned above where precipitation was observed, the amine over phosphate ratio (N/P) was 4/3. This finding suggests that electroneutrality was achieved at this specific ratio, indicating that ca. 3 amines out of 4 per phosphospermine unit were protonated on average at pH 7. Another observation we made here was that the high number of cationic charges did not interfere with base-pairing specificity. We have previously shown that conjugation of a small number of phosphospermine units that provided compounds which remained negatively charged did not affect the ability of the oligonucleotide to discriminate a mismatch.[22,33] Here, single-mismatch discrimination was not addressed, but despite the high number of phosphospermine moieties, conjugates retained their ability to recognize their complementary sequence since they did not form duplexes with unrelated sequences.

For the first time, we have visualized cell entry of the cationic siRNAs. They effectively enter each and every cell on the culture dish. Moreover, a couple of observations support the fact that cationic siRNAs are delivered as single molecules, or at least not as large aggregates. First, the antisense strand cannot be delivered by an unrelated conjugate sequence, showing that proper duplex formation is required. Second, the precipitate generated by the addition of the antisense strand beyond the 1/1 ratio of each strand was inhibiting both cell penetration and activity.

The mechanism of cell entry is not known, although it probably parallels the way cationic vectors carry polynucleotides into cells.[9] Indeed, we show here that cell entry is strictly dependent on the number of phosphospermine units, and the more cationic, the more efficiently conjugated siRNAs enter cells. Fluorescent cationic siRNAs were seen to be distributed with a punctate pattern in the cytoplasm together with some diffuse signal, suggesting endocytosis-mediated cell entry and partial release from vesicles. Since oligonucleotide distribution can be affected by conjugation of a fluorophore, we verified that fluorescently labeled conjugated molecules display the same activity as their nonlabeled counterparts.

The number of phosphospermine units governing solubility and cell delivery, it is not surprising it is also governing gene silencing. While the Z_{20}-conjugate had no activity, gene silencing was already robust for the Z_{25}-conjugated siRNA in the absence of serum. Increasing the number of phosphospermines beyond 25 did not increase activity further, except in the presence of serum where protein binding may interfere. In our first study, similar efficacies were achieved only at a significantly higher Z_{30}-siRNA concentration, which was probably a consequence of poor conjugate purity and hence nondefined heterogeneous mixture following duplex formation. Here, cationic siRNAs are shown to be effective at submicromolar concentrations ranging from 25 to 150 nM, which are much lower than 1−10 μM concentrations reported for lipophilic siRNA, cholesterol−siRNAs or CPP-conjugated siRNAs.[17,34] Nevertheless, active concentrations of cationic siRNAs are still an order of magnitude higher than those used for standard siRNA formulated with a cationic lipid. Cationic lipid/polynucleotides particles have been shown to sediment onto adherent cells in culture and to be completely taken up within 4 h.[35] Yet sedimentation does not occur *in vivo* where particle diffusion is a barrier rather than an advantage. In sharp contrast, Z_{30}-siRNA molecules evenly reach the surface of all cells by Brownian motion, but we do not know how complete this process can be, which makes comparison with particles difficult. In any case, dealing with a molecular drug should lead to a more favorable tissue biodistribution.

Another factor which may be considered is the behavior of phosphospermine-conjugated cationic siRNAs in endosomes with respect to formulated siRNAs into particles. According to the spermine-based structure of the conjugates, their release most probably involves proton sponge-mediated endosome swelling and rupture, as described for polyethylenimine (PEI)[9,36] and lipopolyspermine.[37] However, the intraendoso-

mal concentration of buffering, nonprotonated amines that can be reached with molecules is probably lower than with a particle, the phosphospermine structure offering a lower protonable capacity (1/4, see above) as compared to PEI complexes (ca. 1/2). However, the cell observation after incubation with fluorescent cationic siRNAs indicated the presence of a vesicular pattern and some diffuse signal in the cytoplasm, suggesting that a partial release from endocytotic vesicles occurs. Future investigations are needed to elucidate the mechanism of cell entry of these molecules and their efficacy to escape from endosomes.

Mechanistically, we clearly demonstrated here that cationic siRNAs operate through the RNAi pathway, mediating cleavage of the target mRNA, its subsequent degradation and inhibition of the target protein synthesis. However, the large oligophosphospermine tail may affect the interaction with RISC or limit duplex unwinding. While low internal stability favors unwinding and subsequent activity,[38] phosphospermine conjugation on the contrary increases duplex stability.[21,22] Moreover, the first event facilitating strand dissociation is RISC-mediated cleavage of the sense strand between positions 9 and 10[39−41] and the conjugate might affect this enzymatic cleavage. More work has to be done to address these questions, but if the activity is shown to be affected by conjugation, "second generation" cationic siRNAs containing a cleavable disulfide or ester bond between the siRNA and the polycation could be developed to improve their efficacy. On the positive side, conjugation at the 5′ end of the sense strand should avoid off-target effects triggered by the sense strand.[42]

Finally, the present study was exclusively focused on the conjugated moiety of cationic siRNAs, and data have been obtained using the standard siRNA design as described by Tuschl and collaborators. This means that there is room for improving the activity, by optimizing the sequences or end features. The introduction of modifications in the oligonucleotide part may also enhance the potency.

Cationic siRNAs are less effective than nanoparticles *in vitro*, but this does not hamper their potential as gene silencing drugs *in vivo*. Along this line, an important and even somewhat surprising finding of the present study is that cationic siRNAs remain active in the presence of serum. The slight decrease in activity upon addition of serum is correlated with a decrease in intracellular concentration and may be compensated by increasing the overall positive charge. We further have shown that cationic siRNAs are not degraded in serum-containing culture medium. The oligophosphospermine tail is thus protecting the siRNA against nucleases. It is also responsible for interaction with serum components, among which albumin is the most probable candidate. Albumin is a transport protein for numerous endogenous and exogenous compounds. In support of our hypothesis, albumin has been shown to reversibly bind polyamines and claimed to be their blood carrier.[43,44] Moreover, it improves the half-life of many therapeutically active compounds,[45,46] which is making a hopeful start for our next goal: validate the *in vivo* gene silencing of cationic siRNAs.

■ ASSOCIATED CONTENT

Ⓢ Supporting Information

Supplementary table describing the sequence location of primers and probes used in RT-qPCR. Supplementary Figure 1 showing sequencing traces of the PCR products obtained in the 5′RACE assay. Supplementary Figure 2 showing LaminA/C expression inhibition in HeLa cells following incubation with Z_{25}-laminA/C cationic siRNA. This material is available free of charge via the Internet at http://pubs.acs.org.

■ AUTHOR INFORMATION

Corresponding Author

*Polyplus-transfection, Bioparc, Boulevard S. Brant, 67401 Illkirch, France. E-mail: perbacher@polyplus-transfection.com. Phone: +33 390 406 180. Fax: +33 390 406 181.

Author Contributions

†These authors contributed equally.

Notes

The authors declare no competing financial interest.

■ ACKNOWLEDGMENTS

The authors warmly thank Pascale Belguise (Polyplus-transfection) for the critical reading of the manuscript. This work was supported by Oséo Innovation [A1006001A] and Conseil Régional d'Alsace [A1006001A CR].

■ REFERENCES

(1) Elbashir, S. M.; Harborth, J.; Lendeckel, W.; Yalcin, A.; Weber, K.; Tuschl, T. Duplexes of 21-nucleotide RNAs mediate RNA interference in cultured mammalian cells. *Nature* **2001**, *411* (6836), 494−8.

(2) Ding, S. W.; Voinnet, O. Antiviral immunity directed by small RNAs. *Cell* **2007**, *130* (3), 413−26.

(3) Tomari, Y.; Zamore, P. D. Perspective: machines for RNAi. *Genes Dev.* **2005**, *19* (5), 517−29.

(4) Valencia-Sanchez, M. A.; Liu, J.; Hannon, G. J.; Parker, R. Control of translation and mRNA degradation by miRNAs and siRNAs. *Genes Dev.* **2006**, *20* (5), 515−24.

(5) Berezhna, S. Y.; Supekova, L.; Supek, F.; Schultz, P. G.; Deniz, A. A. siRNA in human cells selectively localizes to target RNA sites. *Proc. Natl. Acad. Sci. U.S.A.* **2006**, *103* (20), 7682−7.

(6) Ohrt, T.; Muetze, J.; Svoboda, P.; Schwille, P. Intracellular localization and routing of miRNA and RNAi pathway components. *Curr. Top. Med. Chem.* **2012**, *12* (2), 79−88.

(7) Robb, G. B.; Brown, K. M.; Khurana, J.; Rana, T. M. Specific and potent RNAi in the nucleus of human cells. *Nat. Struct. Mol. Biol.* **2005**, *12* (2), 133−7.

(8) Juliano, R.; Bauman, J.; Kang, H.; Ming, X. Biological barriers to therapy with antisense and siRNA oligonucleotides. *Mol. Pharmaceutics* **2009**, *6* (3), 686−95.

(9) Behr, J.-P. Synthetic Gene Transfer Vectors II: Back to the Future. *Acc. Chem. Res.* **2012**, *45* (7), 980−4.

(10) Peer, D.; Lieberman, J. Special delivery: targeted therapy with small RNAs. *Gene Ther.* **2011**, *18* (12), 1127−33.

(11) Burnett, J. C.; Rossi, J. J. RNA-based therapeutics: current progress and future prospects. *Chem. Biol.* **2012**, *19* (1), 60−71.

(12) Manoharan, M. Oligonucleotide conjugates as potential antisense drugs with improved uptake, biodistribution, targeted delivery, and mechanism of action. *Antisense Nucleic Acid Drug Dev.* **2002**, *12* (2), 103−28.

(13) Juliano, R.; Alam, M. R.; Dixit, V.; Kang, H. Mechanisms and strategies for effective delivery of antisense and siRNA oligonucleotides. *Nucleic Acids Res.* **2008**, *36* (12), 4158−71.

(14) Soutschek, J.; Akinc, A.; Bramlage, B.; Charisse, K.; Constien, R.; Donoghue, M.; Elbashir, S.; Geick, A.; Hadwiger, P.; Harborth, J.; John, M.; Kesavan, V.; Lavine, G.; Pandey, R. K.; Racie, T.; Rajeev, K. G.; Rohl, I.; Toudjarska, I.; Wang, G.; Wuschko, S.; Bumcrot, D.; Koteliansky, V.; Limmer, S.; Manoharan, M.; Vornlocher, H. P. Therapeutic silencing of an endogenous gene by systemic administration of modified siRNAs. *Nature* **2004**, *432* (7014), 173−8.

(15) Wolfrum, C.; Shi, S.; Jayaprakash, K. N.; Jayaraman, M.; Wang, G.; Pandey, R. K.; Rajeev, K. G.; Nakayama, T.; Charrise, K.; Ndungo,

E. M.; Zimmermann, T.; Koteliansky, V.; Manoharan, M.; Stoffel, M. Mechanisms and optimization of in vivo delivery of lipophilic siRNAs. *Nat. Biotechnol.* **2007**, *25* (10), 1149−57.
(16) Alam, M. R.; Ming, X.; Fisher, M.; Lackey, J. G.; Rajeev, K. G.; Manoharan, M.; Juliano, R. L. Multivalent cyclic RGD conjugates for targeted delivery of small interfering RNA. *Bioconjugate Chem.* **2011**, *22* (8), 1673−81.
(17) Moschos, S. A.; Jones, S. W.; Perry, M. M.; Williams, A. E.; Erjefalt, J. S.; Turner, J. J.; Barnes, P. J.; Sproat, B. S.; Gait, M. J.; Lindsay, M. A. Lung delivery studies using siRNA conjugated to TAT(48−60) and penetratin reveal peptide induced reduction in gene expression and induction of innate immunity. *Bioconjugate Chem.* **2007**, *18* (5), 1450−9.
(18) Muratovska, A.; Eccles, M. R. Conjugate for efficient delivery of short interfering RNA (siRNA) into mammalian cells. *FEBS Lett.* **2004**, *558* (1−3), 63−8.
(19) Turner, J. J.; Jones, S.; Fabani, M. M.; Ivanova, G.; Arzumanov, A. A.; Gait, M. J. RNA targeting with peptide conjugates of oligonucleotides, siRNA and PNA. *Blood Cells Mol. Dis.* **2007**, *38* (1), 1−7.
(20) Moreau, V.; Voirin, E.; Paris, C.; Kotera, M.; Nothisen, M.; Remy, J. S.; Behr, J. P.; Erbacher, P.; Lenne-Samuel, N. Zip Nucleic Acids: new high affinity oligonucleotides as potent primers for PCR and reverse transcription. *Nucleic Acids Res.* **2009**, *37* (19), e130.
(21) Noir, R.; Kotera, M.; Pons, B.; Remy, J. S.; Behr, J. P. Oligonucleotide-oligospermine conjugates (zip nucleic acids): a convenient means of finely tuning hybridization temperatures. *J. Am. Chem. Soc.* **2008**, *130* (40), 13500−5.
(22) Pons, B.; Kotera, M.; Zuber, G.; Behr, J. P. Online synthesis of diblock cationic oligonucleotides for enhanced hybridization to their complementary sequence. *ChemBioChem* **2006**, *7* (8), 1173−6.
(23) Nothisen, M.; Kotera, M.; Voirin, E.; Remy, J. S.; Behr, J. P. Cationic siRNAs provide carrier-free gene silencing in animal cells. *J. Am. Chem. Soc.* **2009**, *131* (49), 17730−1.
(24) Gagnon, K. T.; Watts, J. K.; Pendergraff, H. M.; Montaillier, C.; Thai, D.; Potier, P.; Corey, D. R. Antisense and antigene inhibition of gene expression by cell-permeable oligonucleotide-oligospermine conjugates. *J. Am. Chem. Soc.* **2011**, *133* (22), 8404−7.
(25) Voirin, E.; Behr, J. P.; Kotera, M. Versatile synthesis of oligodeoxyribonucleotide-oligospermine conjugates. *Nat. Protoc.* **2007**, *2* (6), 1360−7.
(26) Haupenthal, J.; Baehr, C.; Kiermayer, S.; Zeuzem, S.; Piiper, A. Inhibition of RNAse A family enzymes prevents degradation and loss of silencing activity of siRNAs in serum. *Biochem. Pharmacol.* **2006**, *71* (5), 702−10.
(27) Westerhuis, W. H.; Sturgis, J. N.; Niederman, R. A. Reevaluation of the electrophoretic migration behavior of soluble globular proteins in the native and detergent-denatured states in polyacrylamide gels. *Anal. Biochem.* **2000**, *284* (1), 143−52.
(28) Kopatz, I.; Remy, J. S.; Behr, J. P. A model for non-viral gene delivery: through syndecan adhesion molecules and powered by actin. *J. Gene Med.* **2004**, *6* (7), 769−76.
(29) Turner, J. J.; Jones, S. W.; Moschos, S. A.; Lindsay, M. A.; Gait, M. J. MALDI-TOF mass spectral analysis of siRNA degradation in serum confirms an RNAse A-like activity. *Mol. Biosyst.* **2007**, *3* (1), 43−50.
(30) McKenzie, J. A.; Grossman, D. Role of the apoptotic and mitotic regulator survivin in melanoma. *Anticancer Res.* **2012**, *32* (2), 397−404.
(31) Mita, A. C.; Mita, M. M.; Nawrocki, S. T.; Giles, F. J. Survivin: key regulator of mitosis and apoptosis and novel target for cancer therapeutics. *Clin. Cancer Res.* **2008**, *14* (16), 5000−5.
(32) Seth, S.; Matsui, Y.; Fosnaugh, K.; Liu, Y.; Vaish, N.; Adami, R.; Harvie, P.; Johns, R.; Severson, G.; Brown, T.; Takagi, A.; Bell, S.; Chen, Y.; Chen, F.; Zhu, T.; Fam, R.; Maciagiewicz, I.; Kwang, E.; McCutcheon, M.; Farber, K.; Charmley, P.; Houston, M. E., Jr.; So, A.; Templin, M. V.; Polisky, B. RNAi-based therapeutics targeting survivin and PLK1 for treatment of bladder cancer. *Mol. Ther.* **2011**, *19* (5), 928−35.
(33) Paris, C.; Moreau, V.; Deglane, G.; Voirin, E.; Erbacher, P.; Lenne-Samuel, N. Zip nucleic acids are potent hydrolysis probes for quantitative PCR. *Nucleic Acids Res.* **2010**, *38* (7), e95.
(34) Petrova, N. S.; Chernikov, I. V.; Meschaninova, M. I.; Dovydenko, I. S.; Venyaminova, A. G.; Zenkova, M. A.; Vlassov, V. V.; Chernolovskaya, E. L. Carrier-free cellular uptake and the gene-silencing activity of the lipophilic siRNAs is strongly affected by the length of the linker between siRNA and lipophilic group. *Nucleic Acids Res.* **2012**, *40* (5), 2330−44.
(35) Barthel, F.; Remy, J. S.; Loeffler, J. P.; Behr, J. P. Gene transfer optimization with lipospermine-coated DNA. *DNA Cell Biol.* **1993**, *12* (6), 553−60.
(36) Boussif, O.; Lezoualc'h, F.; Zanta, M. A.; Mergny, M. D.; Scherman, D.; Demeneix, B.; Behr, J. P. A versatile vector for gene and oligonucleotide transfer into cells in culture and in vivo: polyethylenimine. *Proc. Natl. Acad. Sci. U.S.A.* **1995**, *92* (16), 7297−301.
(37) Labat-Moleur, F.; Steffan, A. M.; Brisson, C.; Perron, H.; Feugeas, O.; Furstenberger, P.; Oberling, F.; Brambilla, E.; Behr, J. P. An electron microscopy study into the mechanism of gene transfer with lipopolyamines. *Gene Ther.* **1996**, *3* (11), 1010−7.
(38) Khvorova, A.; Reynolds, A.; Jayasena, S. D. Functional siRNAs and miRNAs exhibit strand bias. *Cell* **2003**, *115* (2), 209−16.
(39) Leuschner, P. J.; Ameres, S. L.; Kueng, S.; Martinez, J. Cleavage of the siRNA passenger strand during RISC assembly in human cells. *EMBO Rep.* **2006**, *7* (3), 314−20.
(40) Matranga, C.; Tomari, Y.; Shin, C.; Bartel, D. P.; Zamore, P. D. Passenger-strand cleavage facilitates assembly of siRNA into Ago2-containing RNAi enzyme complexes. *Cell* **2005**, *123* (4), 607−20.
(41) Rand, T. A.; Petersen, S.; Du, F.; Wang, X. Argonaute2 cleaves the anti-guide strand of siRNA during RISC activation. *Cell* **2005**, *123* (4), 621−9.
(42) Chen, P. Y.; Weinmann, L.; Gaidatzis, D.; Pei, Y.; Zavolan, M.; Tuschl, T.; Meister, G. Strand-specific 5′-O-methylation of siRNA duplexes controls guide strand selection and targeting specificity. *RNA* **2008**, *14* (2), 263−74.
(43) Beauchemin, R.; N'Soukpoe-Kossi, C. N.; Thomas, T. J.; Thomas, T.; Carpentier, R.; Tajmir-Riahi, H. A. Polyamine analogues bind human serum albumin. *Biomacromolecules* **2007**, *8* (10), 3177−83.
(44) Dubeau, S.; Bourassa, P.; Thomas, T. J.; Tajmir-Riahi, H. A. Biogenic and synthetic polyamines bind bovine serum albumin. *Biomacromolecules* **2010**, *11* (6), 1507−15.
(45) Elsadek, B.; Kratz, F. Impact of albumin on drug delivery - New applications on the horizon. *J. Controlled Release* **2012**, *157* (1), 4−28.
(46) Kratz, F. Albumin as a drug carrier: design of prodrugs, drug conjugates and nanoparticles. *J. Controlled Release* **2008**, *132* (3), 171−83.